Journal of Chemical Health Risks
www.jchr.org
JCHR (2024) 14(1), 3293-3307 | ISSN:2251-6727

DNA Binding, Photo Cleavage Mechanism and in Silico Docking Studies of 1,3,4-Oxadiazole Schiff's Base Derivatives, Their Synthesis and Characterization

Ravindra Devidas Patil[1], Dr. Sujata F. Harlapur[2], Dr. Shridhar A. H.[3]

[1]Asst. Professor, Department of Chemistry, Faculty of Science, Sigma University, Vadodara, Gujarat 390019, India. & Visvesvaraya Technological University, Jnana Sangama, Machhe, Belgaum, Karnataka 590018, India.

[2]Professor & Head of Department, Department of Chemistry, Vemana Institute of Technology, VTU, Bangalore 560064, India.

[3]Assistant professor, Department of Chemistry, SVM Arts Science & Commerce Degree college Ilkal, Dist. Bagalkot, Karnataka 587125, India.

(Received: 27 October 2023 Revised: 22 November Accepted: 26 December)

KEYWORDS

Oxadiazole Schiffs base, in silico docking, DNA binding, DNA cleavage, in silico acute toxicity.

ABSTRACT:

The present study emphasizes on the synthesis and biological activity of the 1,3,4- substitute Schiffs base derivatives 5(a-f). In silico docking studies were performed to analyse the efficiency of the synthesized compounds for their antimicrobial, DNA binding cleavage potential and acute toxicity properties. Results of the study highlight that the compounds 5c, 5a, and 5e are comparatively more significant bioactive molecules among the synthesized compounds with minimal toxic effects. Further, the hypothesis of the docking studies was evaluated by in vitro antimicrobial, and the DNA binding cleavage efficiency of the synthesized compounds 5(a-f) with Circulating Tumour DNA (CT-DNA) was examined through UV absorption and viscosity measurement studies. The study results reveal that the compound firmly binds via interactive mode with CT-DNA and provides a distinctive DNA binding pattern. The study results justified the hypothesis made through docking and proved it as a potent bioactive molecule.

Graphical Abstract

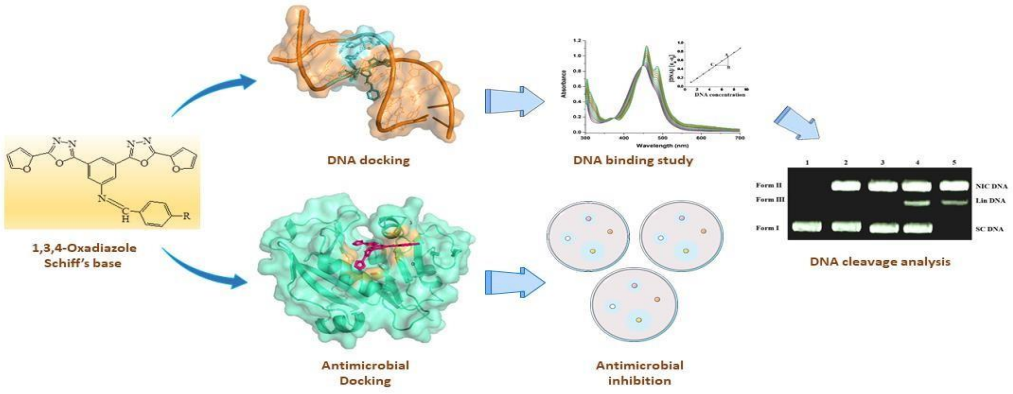

1. Introduction

Heterocycles are compounds that cover a more significant part of the organic compounds, possessing their own importance in the therapeutic and pharmaceutical molecules. It is noticed that drug has to undergo effective interaction with the organism to inhibit further growth and efficiently control their action. Hence, there is ample opportunity for the researcher to strengthen the discovery of drugs to bind effectively and control action, even against the organisms that have developed resistance towards a drug used to treat infection caused by them.

Journal of Chemical Health Risks
www.jchr.org
JCHR (2024) 14(1), 3293-3307 | ISSN:2251-6727

1,3,4- oxadiazole is such a class of organic compounds bearing oxygen, nitrogen atoms are found many effective molecules as a therapeutic agent to teat agents the various disease caused by the micro-organism [1]. Oxadiazole exhibits a wide range of the biological spectrum by its mode of interaction through hydrogen bonding with receptors [2]. 1,3,4 - oxadiazole molecules are known for their action as an antimicrobial [3], anti-inflammatory [4], anti-cancer [5], cytotoxic [6] DNA binding [7], and found to be a potent bioactive molecule with lower toxicity effect [8]. Further literature survey reveals that biological activity of the oxadiazole enhanced by incorporating Schiff's bases which contains toxophoric C=N linkage in them [9]. A report on the oxadiazole Schiffs base disclosed their action as an effective bioactive molecule [10]. Hence bases on the above findings and in quest of our interest in search and development of the biologically active molecules stimulated to synthesized new series 1,3,4-oxadiazole fuse Schiffs base derivatives. The study efficiency of the synthesized for their bioactive property in-silico docking study was done, and the outcome of the study reveals compounds are potent bioactive molecules.

Further to evaluate the theoretical hypothesis by in-silico docking, synthesis compounds were tested for their in-vitro antimicrobial against gram-positive, gram-negative bacteria and fungi. DNA binding and photocleavage studies were conducted to study interaction molecules. Results of the study support the theatrical hypothesis and are proved as a potent bioactive compound. The structure of the newly synthesized compound was confirmed by IR, NMR, and Mass Spectral studies, and results are found in good agreement with molecular structure.

2. Materials and Methods

All analytical grade chemicals were used directly. Melting points were determined in the scientific melting point apparatus and uncorrected. The progression of the reaction was observed by TLC using silica gel coated plates (0.5 mm thickness, Merck), and spots were viewed under the UV chamber. Compounds prepared were purified by recrystallization method using a suitable solvent. The structure was confirmed by recording Infra-Red spectra in the Perkin Elmer-spectrum RX-1model spectrophotometer. NMR spectra were recorded by Bruker DRX500 MHz spectrometer using DMSO as a solvent and TMS as an internal reference. Mass spectra were recorded using PerkinElmer NexION 1000 ICP Mass Spectrometer.

2.1. Synthesis of Schiffs base 5(a-f)

Compound 1 and 2 were synthesized by the reported method [13]

4.1.1. Synthesis of 2,2'-(5-nitrobenzene-1,3-diyl) bis[5-(furan-2-yl)-1,3,4-oxadiazole] (**3**)

5-nitrobenzene-1,3-dicarbohydrazide (1 mmol) and furan- 2- carboxylic acid (2 mmol) were taken in a round bottom flask to this POCl+ (10 mL) was added slowly. Further, the content was refluxed for about 6-8 hrs. once the reaction is completed mixture was allowed to cool to attain room temperature. Then the reaction mixture slowly poured into ice-cold water. The solid obtained was neutralized with anhydrous sodium bicarbonate and filtered. The solid obtained was dried and purified by recrystallization in ethanol.

2.1.2. General procedure for the synthesis of 3,5-bis[5-(furan-2-yl)-1,3,4-oxadiazol-2-yl] aniline (**4**)

2,2'-(5-nitrobenzene-1,3-diyl)bis[5-(furan-2-yl)-1,3,4-oxadiazole] (1 mmol) obtained from the previous step and $SnCl_2.2H_2O$ (5 mmol) was taken in a round bottom flask then dissolved by the addition of 0.02 M methanolic HCl solution further contain were refluxed for 3-4 hrs at 70-80 0C my maintaining nitrogen atmosphere condition. The reaction mixture was concentrated under reduced pressure. After the completion of the reaction, the product obtained was diluted with ethyl acetate and then washed with aq. $NaHCO_3$ and water and then spectated using a separating funnel. The organic layer obtained was dried over anhydrous sodium sulphate, then concentrated and recrystallized from methanol.

2.1.3. Synthesis of Bis 1,3,4-oxadiazole substituted Schiffs base **5(a-f)**

Compound 3,5-bis[5-(furan-2-yl)-1,3,4-oxadiazol-2-yl] aniline (**4**) obtained (1 mole) taken in the round bottom flask fitted with water cool condenser. Then compound is dissolved using methanol, to this content substituted aldehyde (1mole) was added slowly with constant stirring till completion of addition. To this 4 mL of glacial acetic acid were added. Further the reaction mixture was refluxed for 8 to 10 Hrs. progress of the

Journal of Chemical Health Risks
www.jchr.org
JCHR (2024) 14(1), 3293-3307 | ISSN:2251-6727

reaction was monitored by using TLC. After the completion of the reaction the content was transferred into ice cold water. The precipitate obtained was filtered, washed water and dried. Further obtained compound was recrystalized by using methanol.

2.2. In silico Docking Studies

2.2.1. In silico Acute Oral Toxicity prediction

Acute oral toxicity (AOT) studies were carried out to analyze the short-term adverse events of a chemical compound (drug) when a statistically devised single or multiple doses are administered over a period of time in two mammalian species. Acute toxicity studies give insights into the probable acute toxicity in the animals used by the estimation of the safe acute doses [14]. In order to execute a classical LD50 acute toxicity study, the laboratory mice and rats are usually sacrificed. As a step to reduce the animal sacrifice for the acute toxicity experiments, novel in silico based tools and servers based on the various mathematical models and statistical methods have been developed.

Machine learning-based methods are gaining potential in the field of in silico-based toxicity prediction based on the qualitative classification, and further quantitative regression predictive models have ranked these methods as an alternative means for lead optimization [15]. A DL-AOT prediction server is a web-based tool developed based on a Deep learning framework comprising multiple layered convolution neural networks. It works based on the consensus regression model (deepAOT-R), which can perform multiple classifications based on the deepAOT-C model [16]. Its prediction potential has been calculated using 1673 and 375 compound test sets separately. The R2 and MAE calculated values for the first test set were 0.864 and 0.195 based on deepAOT-R. The accuracy percentage of the deepAOT-C model was 95.5% and 96.3% for both the test sets (set1 and set2), which exhibited an advanced level among the AOT prediction tools. DL-AOT accepts input files in "*.smi", "*.mol", "*.mol2", "*.sdf" formats and the model type “Regression model and multi-class model” was selected for the prediction of **5a-5f** molecule’s acute toxicity. The evaluated toxicity levels are denoted with symbols and descriptions (1. danger/poison 2. warning 3. Caution and 4. none required).

2.2.2. In silico DNA Interaction Analysis

Dihydrofolate reductase (DHFR) is involved in the catalysis of the reduction reaction of dihydrofolate to tetrahydrofolate (THF). THF is essential for the activity of folate-dependent enzymes in the folate biosynthetic pathway leading to DNA synthesis and methylation. In the earlier studies, DHFR has been validated as the crucial target to inhibit the activity of Candida albicans [17,18].

Docking studies targeting the biomolecules, including the DNA with the newly synthesized ligands, is very significant as it is a crucial step to explore the specific activity and binding potential of the synthesized ligands with the biomolecules, which leads to the advancement in biomedical research with special emphasis to anticancer drug design and development. Earlier studies [19-21] have reported the in silico docking studies to cross-verify the results obtained in the in vitro experiments.

DNA gyrase (gyrB) is involved in the initiation of DNA replication and the elongation process of the newly formed DNA strand. gyrB (B. subtilis and P. aeruginosa) have been validated as the antibacterial drug target leading to multiple antibiotic resistance in the earlier studies based on catalytic site and multi-prospective binding sites [22, 23]. Furthermore, the ATP-binding sites are highly conserved in gyrB, and these have been ranked as potential candidate drug targets for the design and development of novel broad-spectrum antibacterial drugs [24, 25].

2.2.3. In silico antimicrobial analysis

The docking simulation study was carried out to know the binding potential between the ligand molecules 5 (a-f) and DHFR (PDB ID: 1AI9_B) (C. albicans); gyrB (B. subtilis and P. aeruginosa). The PDB structures of the protein targets were searched using BLASTp and retrieved from the RCSB PDB database. PDB structures with PDB IDs 2WYC_B (1.90 Å) and 1AI9_B (2.30 Å) were retrieved with .pdb extension. Due to the non-availability of the gyrB (B. subtilis), 3D structure was modeled using SWISS-MODEL [26], the selected model was further refined using Galaxy Refine [27], and structure analysis was assessed using Ramachandran plot analysis (PROCHECK) [28]. The proteins were submitted to the PyRx program to execute the docking procedure based on AutoDock vina [29] for the docking studies. The ligand molecular structures (5a-5f) were drawn using Marvin sketch, and the structures were

Journal of Chemical Health Risks
www.jchr.org
JCHR (2024) 14(1), 3293-3307 | ISSN:2251-6727

downloaded as .sdf files. Open Babel was employed for the Energy minimization procedure [30].

Further, the grid box was set to target protein structures specifically based on the x, y and z coordinates (34.76, 38.03 & 37.58 (model, B. subtilis); 37.16, 46.72 & 41.76 (2WYC_B);
10.15, 30.47 & 18.80 (1AI9)) respectively. The grid box dimensions were set as (31.12, 31.12

& 31.12 (model, B. subtilis); 22.06, 24.02 & 23.37 (2WYC_B); 28.74, 28.74, & 28.74

(1AI9_A)) in the x, y and z-axis respectively covering the binding sites of the proteins within the grid box. The grid box was set for the DNA docking procedure with grid box dimensions (25.00, 25.00 & 29.89 (1BNA)) for x, y, and z-axis correspondingly placing the DNA molecule well within the grid box.

The binding affinity of the docked complexes (protein-ligand interaction) was prioritized based on the lowest docking scores (AutoDock scores) and was further visualized precisely using PyMOL 2.4 [31], and the 2D plots (Target-ligand interactions) were generated to examine the interactions using LigPlot+ [32].

2.3. In vitro Antimicrobial Activity

2.3.1 Determination of minimal inhibitory concentrations (MIC)

For evaluation MIC of the synthesized compounds agar dilution susceptibility method by following modified method of Clinical and Laboratory Standards Institute 2012. 5% stock solution was prepared by dissolving test compounds **5(a-f)** sterilized DMSO solution (400 mg/mL). Further solution prepared was serially diluted to different concentration of 40, 20, 10, 5, and 2.5 mg/mL in nutrient agar for bacterial and potato dextrose agar for fungi. Solution prepared were poured in to a Petridis then solidified. After solidification of the solution, plates were spotted with 100 µL of overnight grown bacterial cultures approximately containing 1×104 CFU/mL. 18-24 hrs Incubation is done ate 37°C for bacterial culture and incubation of 24 - 48 hrs at 24 °C for fungal cultures was done determine the MIC of synthesized compounds [33].

2.3.2 Antimicrobial screening

The antimicrobial efficiency of the synthesized compounds 5 (a-f) was determined by in vitro antimicrobial method, against Gram-positive bacteria Staphylococcus aureus, Bacillus subtilis Gram-negative bacteria Bacillus subtilis Pseudomonas aeruginosa, Escherichia coli, and two fungi Candida albicans, Candida parapsilosis. In order to determine antimicrobial property of synthesized compounds standard serial dilution method adopted by taking a stock solution of dilution 100 g/ml [34]. The identified clinical isolates were collected following the standard method. Efficiency of the synthesized compound were compared with standard drugs Ampicillin for bacterial and fluconazole fungi.

Evaluation of the antimicrobial activity was performed by sensitive agar well radial diffusion technique [35]. Nutrient agar medium and potato dextrose agar medium prepared wase sterilized and spread on sterilized Petri dishes separately for bacterial and fungal culture. 24 hrs incubation is done for the 100 µL clinical isolates contain Nutrient broth cultures. And 48 hrs of incubation was done for fungal cultures nutrient potato dextrose agar medium culture. Further 100 µL of standard ampicillin drug is loaded in to their corresponding wells of bacterial culture plates followed by 20 µL of test compounds was loaded in the corresponding well prepared for test sample. For antifungal activity 100 µL standard fluconazole drug and 20 µL of test compounds were loaded on to their corresponding wells prepared in the fungal culture plates. The sample and standard drug loaded in bacterial plates were incubated for 24 hrs at 37 °C similarly fungal plates were incubated for 48 hrs at 24°C. after incubation the zone of complete inhibition of both bacteria and fungi was measured and recorded in mm. The results of these experiments are expressed as mean ± S.E.M. of three replicates in each test.

2.4. DNA binding studies (Electronic absorption titration)

Mode of binding interaction of the synthesized molecule **5b,5d and 5g** with DNA helix were studied with absorption spectroscopic method which is found to be more constructive approach. Electronic absorption study reveals that maximal absorption intensity showed 280nm by the synthesized ligand molecules (**5b,5d and 5g**) which containing multiple bonds in the moiety which leads to $\pi \rightarrow \pi^*$ transitions, as illustrated in **Figure 4-6**. Compound were tested by increasing concentration of the DNA (5mM Tris HCl/50mM NaCl) which was taken in buffer solution, 'hypochromism' which is designated as red shift was observed which leads to the decrease in the absorption intensity of intra ligand

Journal of Chemical Health Risks
www.jchr.org
JCHR (2024) 14(1), 3293-3307 | ISSN:2251-6727

absorption, which exhibits the active effective interaction of chromophore functional group of the molecule with DNA base pairs. The spectroscopic analysis magnifies the greater binding affinity and interaction of the molecules through its hypochromism for intercalative interactions with DNA [36, 37].

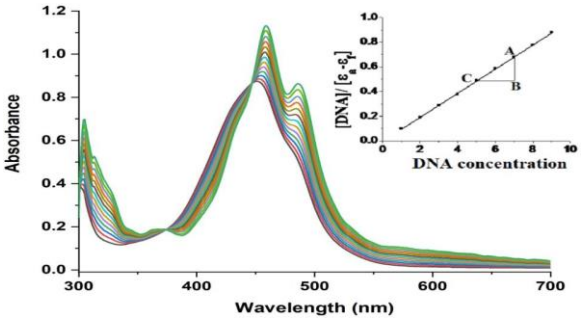

Figure 4. The absorption spectra of **5b** in Tris–HCl buffer upon addition of DNA. Complexes = 0.5 mM, [DNA] = 0-100 μM. Inner graph of [DNA]/ ($\square_a$-$\square_f$) vs. [DNA] for titration of DNA with metal complexes.

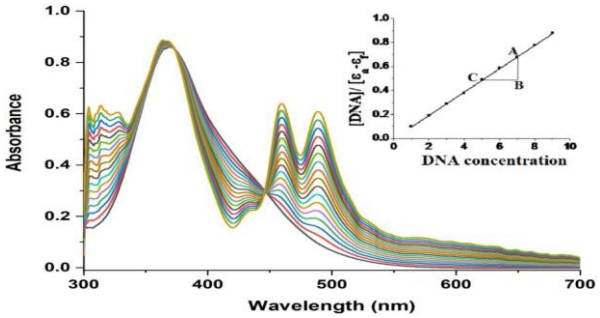

Figure 5. The absorption spectra of **5d** in Tris–HCl buffer upon addition of DNA. Complexes = 0.5 mM, [DNA] = 0-100 μM. Inner graph of [DNA]/ ($\square_a$-$\square_f$) vs. [DNA] for titration of DNA with metal complexes.

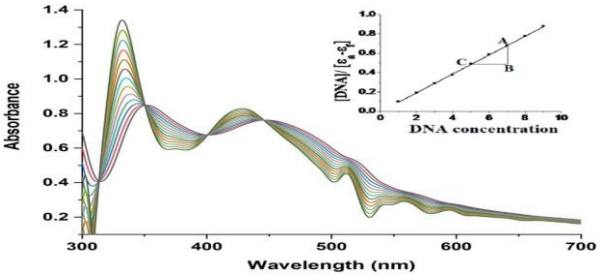

Figure 6. The absorption spectra of **5g** in Tris–HCl buffer upon addition of DNA. Complexes = 0.5 mM, [DNA] = 0-100 μM. Inner graph of [DNA]/ ($\square_a$-$\square_f$) vs. [DNA] for titration of DNA with metal complexes.

Absorption of **5b**, **5d**, and **5g** with CT-DNA measured to investigate the characteristic binding property of the synthesized compound 5(b-g), having intrinsic binding constants Kb with CT-DNA. The intrinsic binding constants (Kb) of the corresponding compounds were found to be 2.9×104 M-1, 2.6×104 M-1, and 1.4×104 M-1. This result exhibits the binding of the compounds with CT-DNA with an order of **5g** > **5b** > **5d.** Further planarity of the interacting molecules plays an immense role in the further continuous interaction of compound with CT-DNA. The results are found similarity in intercalator with the above compounds point outs primary molecules substituents difference in binding constants Kb.

2.5. DNA cleavage activity

Compounds (**5b-g**) were analysed for the plasmid pUC19 DNA cleavage assays by adopting reported agarose gel electrophoresis method to probe the DNA cleavage activities. maintaining anaerobic conditions maintained and observed for supercoiled DNA (Form I) to nicked DNA (Form II) and linear DNA (Form III) to investigate the DNA cleavage. Control taken for the analysis which does not contain the test sample does not shown any cleavage of the DNA (lane 1). Results of the Similar study made by considering compounds **5(b-g)** leads to the cleavage of the apparent plasmid DNA at concentration of 50 μM. At higher concentration DNA cleavage can be made very efficiently (lanes 3-5) as depicted in **Figure- 7.**

Transformation of supercoiled DNA from Form I to III that is nicked and linear form of pUC19 DNA made enable at a concentration of 50 μM. It has been observed with increase in the concentration of the compound's magnitude of form I pUC19 DNA decreased regularly (lanes 3 and 4), but there is an increase in the intensity with form III. Much significant cleavage ability exhibited by the compound 5g with pUC19 DNA. And also, it is having an ability to convert up to 75% of DNA from the form I to III at a concentration of 50 μM. Compound 5b at a concentration of 50 μM found to be much efficient (lane 4) which is capable to transform supercoiled pUC19 DNA to form II and form III. This study shows among the compound investigated for the DNA-cleavage property, compound 5g found much effective nuclease mimic compared to the 5b and 5d. The different DNA-cleavage competence of the two compounds may be examined because of the distinct binding ability of the compounds to DNA [38.39].

Journal of Chemical Health Risks
www.jchr.org
JCHR (2024) 14(1), 3293-3307 | ISSN:2251-6727

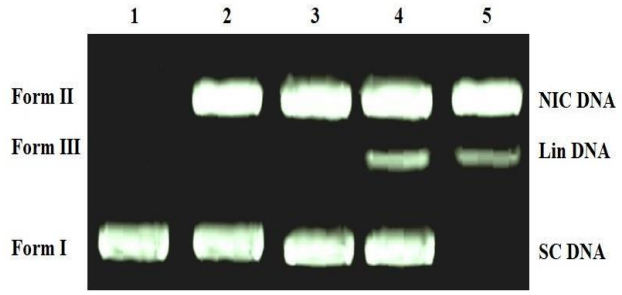

Figure 7: Effects of 5b/5d/5g compounds at same concentrations (50 µmol/L) on the pUC 19 supercoiled DNA against OH generated by photolysis at 360 nm for 30 min. Lane 1, Untreated DNA (control); lane 2, DNA + H_2O_2; lane 3, DNA + 5b (50 µmol/L); lane 4, DNA + 5d (50 µmol/L); lane 5, DNA + 5g Complex (50 µmol/L).

3. Results and Discussion

3.1. Chemistry

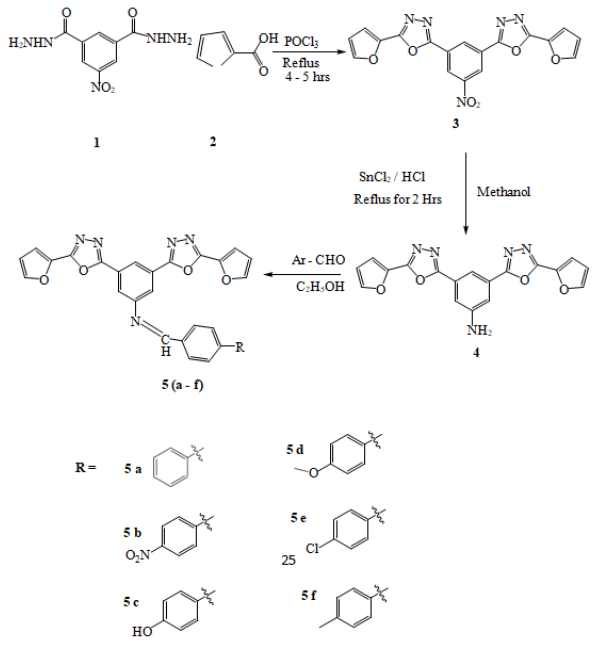

Scheme -1. Synthesis of 1,3,4-Oxadiazole Schiff's base derivative

As depicted in **scheme-1**, 1, 3, 4-oxadiazole based Schiffs base derivatives were prepared by multi steps reaction. In the IR spectrum of compounds absorption peak at 1673 (C =N Stretching), cm-^{1} indicates the C=N of the Schiffs base, a peak at 1262 cm^{-1} due C-O Stretching of the furan ring. and peak at 1200 to 1350 cm^{-} NMR spectra at δ ppm: 8.7 represents presence of CH attached C=N, δ ppm: 6-7 aromatic protons of oxadiazole ring and δ ppm 7.4 -7.6 for the substituted aldehydes. LCM data obtained (in positive mode) confirms the molecular mass of the synthesized compounds.

3.2. Physical and Spectral data of synthesized compounds

3.2.1. (Z)-N-benzylidine -3,5—bis(5-furan-2-yl)-1,3,4-oxadiazol-2-yl)benzenamine (5a) Pale yellow colour solid; Yield 57%, MP 126 ^{0}C; IR spectrum: 2926 Cm^{-1} (C-H Stretching), 1778 Cm^{-1} (C=C stretching), 1673 (C =N Stretching), 1262 (C-O Stretching); ^{1}H NMR (DMSO_d6, 500 MHz) δ ppm: 8.7 (s, 1H, CH attached C=N), 7.6 (s, 1H, Ar-CH),7.4 (d, 2H, Ar-CH),7.3 (m,3H Ar-H),6.9 (m, 4H, Ar-H), 6.5 (m, 4H, Ar-H); ^{13}C NMR (DMSO_d6, 500 MHz): 163.8 (2C,C = N of oxadiazole ring), 161.6 (1C,C = N),158.4 (2C, N=C of oxadiazole ring), 145.3 (2C,C-O of furan ring), 142.6 (2C,C-O of furan ring), 132.4 (1C, C-N of benzene ring), 131.2 (1C, C=C of benzene ring),129.3 (2C,C=C of benzene ring),126.1 (2C, C=C of benzene ring), 108.3 (2C, C=C of furan ring), 104.7 (2C, C=C of furan ring); LCMS m/z 451.2 (M+) (100); anal. calcd. for $C_{25}H_{15}N_5O_4$ (%): C, 66.81; H, 3.36; N, 15.58; O, 14.24

found: C, 66.32; H, 3.46; N, 15.62; O, 14.27

3.2.2. (Z)-N-(4-nitrobenzylidene)-3,5-bis(5-(furan-2-yl)-1,3,4-oxadiazol-2-yl benzenamine (5b) Yellow colour solid; Yield 62 %, MP 147 ^{0}C; IR spectrum: 2923 Cm^{-1} (C-H Stretching), 1769 Cm^{-1} (C=C stretching),1673 (C =N Stretching), 1562 and 1348 (N–O Stretching of Niro group),1262 (C-O Stretching); ^{1}H NMR (DMSO_d6, 500 MHz) δ ppm: 8.3 (s, 1H, CH attached C=N), 8.1 (d, 2H, Ar-CH), 7.9 (d,2H Ar-H),7.6 (s, 1H, Ar-CH), 7.1 (m, 4H, Ar-H),
6.2 (m, 4H, Ar-H); ^{13}C NMR (DMSO_d6, 500 MHz): 163.8 (2C,C = N of oxadiazole ring),

161.2 (1C,C = N),157.7 (2C, N=C of oxadiazole ring), 153.9 (1C, N-C), 150,6 (1C, C- N of

NO_2),147.1 (2C,C-O of furan ring), 141.8 (2C,C-O of furan ring), 138.7 (1C, C-N of benzene

ring), 130.6 (2C, C=C of benzene ring),122.3 (2C,C=C of benzene ring),124.1 (1C, C=C of benzene ring), 106.4 (2C, C=C of furan ring), 106.3 (2C, C=C of

Journal of Chemical Health Risks
www.jchr.org
JCHR (2024) 14(1), 3293-3307 | ISSN:2251-6727

furan ring); LCMS m/z
493.6 (M+) (100); anal. calcd. for $C_{25}H_{14}N_6O_6$ (%): C, 60.73; H, 2.85; N, 17.00; O, 19.42

found: C, 60.34; H, 2.63; N, 17.27; O, 19.56.

3.2 .3. (Z)-N-(3,5—bis(5-furan-2-yl)-1,3,4-oxadiazol-2-yl)phenylamino)methyl)phenol (5c)

White colour solid; Yield 68 %, MP 127 ^{0}C; IR spectrum: 3648 (O-H Stretching), 2932 Cm^{-1} (C-H Stretching), 1776 Cm^{-1} (C=C stretching), 1687Cm^{-1} (C=N stretching),1267 (C-O Stretching); ^{1}H NMR (DMSO_d6, 500 MHz) δ ppm: 8.2 (s, 1H, CH attached C=N) ;7.8 (1H, Ar-CH), 7.3 (d,2H Ar-H), 7.4(m, 4H, Ar-H), 6.8 (d, 2H, Ar-H), 6.4 (m, 4H, Ar-H), 4.6 (1H, -OH) ; ^{13}C NMR (DMSO_d6, 500 MHz): 164.4 (2C,C = N of oxadiazole ring), 160.8 (1C,C = N), 159.7 (1C , Ar - C-OH),157.2 (2C, N=C of oxadiazole ring), 154.5 (1C, N-C), 147.8
(2C,C-O of furan ring), 142.6 (2C,C-O of furan ring), 130.2 (2C, C=C of benzene ring),

126.2 (1C, C-N of benzene ring), 128.3 (2 C, Ar C of Benzene ring), 124.3 (1C, C=C of benzene ring),122.2 (2 C, Ar C of Benzene ring), 116.3 (2C,C=C of benzene ring), 107.2 (2C, C=C of furan ring), 105.3 (2C, C=C of furan ring); LCMS m/z 493.6 (M+) (100); anal. calcd. for $C_{25}H_{15}N_5O_5$ (%): C, 64.52; H, 3.25; N, 15.05; O, 17.19 found: C, 64.32; H, 3.27; N,
15.18; O, 17.29.

3.2.4.(Z)-N-(4-methoxybenzylidine-3,5—bis(5-furan-2-yl)-1,3,4-oxadiazol-2yl) benzenamine (5d)

White colour solid; Yield 68 %, MP 168 ^{0}C; IR spectrum: 2938 Cm^{-1} (C-H Stretching), 1764 Cm^{-1} (C=C stretching), 1687Cm^{-1} (C=Stretching), 1327 (C-O Stretching); ^{1}H NMR (DMSO_d6, 500 MHz) δ ppm: 8.3 (s, 1H, CH attached C=N) ;7.8 (1H, Ar-CH), 7.6 (d,2H Ar-H), 7.5 (m, 4H, Ar-H), 6.9 (d, 2H, Ar-H), 6.2 (m, 4H, Ar-H), 3.7 (3H, -OCH3) ; ^{13}C NMR (DMSO_d6, 500 MHz): 164.2 (2C,C = N of oxadiazole ring), 163.2 (1C,C -O), 160.3 (1C,C= N), 157.6 (2C, N=C of oxadiazole ring), 154.3 (1C, N-C), 147.3 (2C,C-O of furan ring),

142.9 (2C,C-O of furan ring), 130.5 (2C, C=C of benzene ring), 128.2(1C, C-N of benzene ring), 126.4 (2 C, Ar C of Benzene ring), 121.7 (2C, C=C of benzene ring),114.2 (2 C, Ar C of Benzene ring) 107.6 (2C, C=C of furan ring), 105.6 (2C, C=C of furan ring)56.2 (3C, O- CH_3) ; LCMS m/z 481.3 (M+) (100); anal. calcd. for $C_{26}H_{17}N_5O_5$ (%): CC, 65.13; H, 3.57; N,
14.61; O, 16.69 found: C, 65.23; H, 3.61; N, 14.38; O, 16.83.

3.2.5.(Z)-N-(4-chlorobenzylidene)-3,5-bis(5-(furan-2-yl)-1,3,4-oxadiazol-2-yl) benzenamine

(5e)
Pale yellow colour solid; Yield 68 %, MP 153 ^{0}C; IR spectrum: 2942 Cm^{-1} (C-H Stretching), 1764 Cm^{-1} (C=C stretching), 1687Cm^{-1} (C=Stretching), 1327 (C-O Stretching), 832 (Ar-Cl Stretching); ^{1}H NMR (DMSO_d6, 500 MHz) δ ppm: 8.2 (s, 1H, CH attached C=N) ;7.6 (1H, Ar-CH), 7.5 (d,2H Ar-H), 7.4 (m, 4H, Ar-H), 7.1.9 (d, 2H, Ar-H), 6.4(m, 4H, Ar-H) ; ^{13}C NMR (DMSO_d6, 500 MHz): 164.6 (2C,C = N of oxadiazole ring), 160.7 (1C,C = N), 157.2
(2C, N=C of oxadiazole ring), 154.7 (1C, N-C), 147.8 (2C,C-O of furan ring), 142.3 (2C,C- O of furan ring), 132.1 (1C, C=C-C of benzene ring), 130.7 (2C, C=C of benzene ring),
129.3 (2 C, Ar C of Benzene ring), 128.6 (2C, Ar C of Benzene ring), 121.4 (2C, C=C of benzene ring), 107.4(2C, C=C of furan ring), 105.3 (2C, C=C of furan ring) ; LCMS m/z
485.1 (M+) (100); anal. calcd. for $C_{25}H_{14}ClN_5O_4$ (%): C, 62.06; H, 2.92; Cl, 7.33; N, 14.47;

O, 13.23 found: C, 62.23; H, 2.97; Cl, 7.46; N, 14.52; O, 13.28.

3.2.6.(Z)-N-(4-methylbenzylidine-3,5-bis(5-furan-2-yl)-1,3,4-oxadiazol-2-yl) benzenamine

(5f)

White colour solid; Yield 68 %, MP 173 ^{0}C; IR spectrum: 2948 Cm^{-1} (C-H Stretching), 1763 Cm^{-1} (C=C stretching), 1686Cm^{-1} (C=Stretching), 1348 (C-O Stretching); ^{1}H NMR (DMSO_d6, 500 MHz) δ ppm: 8.3 (s, 1H, CH attached C=N) ,7.6 (1H, Ar-CH), 7.5 (d,2H Ar-H), 7.3 (m, 4H, Ar-H), 7.1 (d, 2H, Ar-H), 6.4 (m, 4H, Ar-H), 2.5 (3H, -CH_3) ; ^{13}C NMR (DMSO_d6, 500 MHz): 164.3 (2C,C = N of oxadiazole ring), 160.4 (1C,C = N), 157.6 (2C,
N=C of oxadiazole ring), 154.3 (1C, N-C), 147.3 (2C,C-O of furan ring), 142.7 (2C,C-O of furan ring), 130.1 (1C, C=C-C of benzene ring), 130.7 (2C, C=C of benzene ring), 129.3 (2 C, Ar C of Benzene ring), 129.4 (2C, Ar C of Benzene ring), 129.47(2C, C=C of benzene ring), 107.6(2C, C=C of furan ring), 105.1 (2C,

Journal of Chemical Health Risks
www.jchr.org
JCHR (2024) 14(1), 3293-3307 | ISSN:2251-6727

C=C of furan ring) 26.2 (3C, -CH_3) ; LCMS m/z 481.3 (M+) (100); anal. calcd. for $C_{26}H_{17}N_5O_4$ (%): C, 67.38; H, 3.70; N, 15.11; O, 13.81
found: C, 67.26; H, 3.74; N, 15.37; O, 13.85.

3.3. In silico Docking Studies

3.3.1. In silico Docking analysis of anti-microbial action

To perform the docking studies of the **5a-5f** ligand molecules suggested to be the potential antimicrobial inhibitors in the in vitro experimenta results against C. albicans, B. subtilis and P. aeruginosa and were considered for in silico docking simulation analysis. DHFR (PDB ID: 1AI9_B) was selected as the antifungal target (C. albicans) to perform binding affinity analysis using AutoDock vina 4.2. The docking simulation results exhibited significant interactions with the ligand **5a** with docking energy -6.9 Kcal/mol interacting with residues (ARG-34 (3.16 Å) and PHE-66 (3.16 Å)), forming two H-bonds and nine Vander Waals interactions shown in **Fig. 1**.

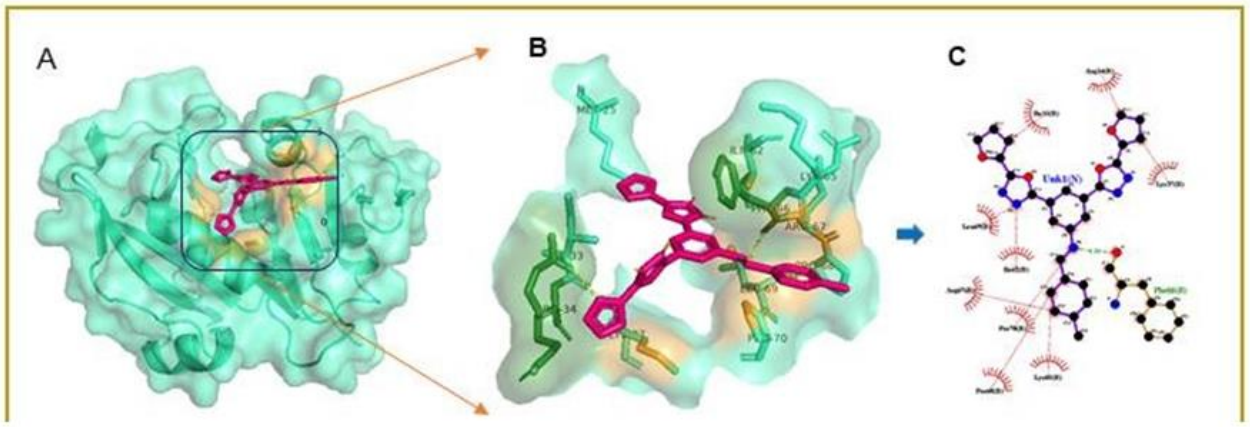

Figure 1. Illustrates the interaction between **5a** with (A) (1AI9_B) (greencyan), (D) (modeled protein) (marine) &(G) (2WYC_B) (olive); B, E & H (ligand **5a** (hotpink, forest & red), interacting binding site residues); (C, F & I) (2D plots of protein-**5a** interaction with H-bonds and Vander-Waals interactions).

gyrB (B. subtilis), being a well-studied antibacterial target, was selected as a target protein, docking studies were carried out to analyze the binding mode of the gyrB (protein model) and the ligands **5a-5f**. The docking results obtained strongly revealed the potential binding affinity with the highest binding score -10.8 Kcal/mol between the protein target and ligand **5a**, docking results are as shown in **Table 1**. Four H-bonds were formed with interacting residues ((HIS-118 (2.99 Å), GLU-602 (2.93 Å) and ASP-603 (3.30 Å; 2.90 Å)) and fourteen Vander Waals interactions were recorded.

Table 1 Illustration of the AutoDock Vina binding energy scores of **5(a-f)** against respective targets microorganisms.

Microorganisms	**Binding Energy (kcal/mol) at rmsd/ub=0 & rmsd/lb=0**							
	5a	**5b**	**5c**	**5d**	**5e**	**5f**	**Ampicillin**	**Fluconazole**
Candida albicans (1AI9_B)	-6.9	-6.6	-6.8	-6.9	-6.6	-7.1	--	-6
Pseudomonas Aeruginosa (2WYC_B)	-8.6	-8.6	-8.6	-8.6	-8.	-8.8	-7.1	--
Bacillus subtilis (Modeled protein)	-10.8	-9.9	-10.7	-10	-10.2	-10.1	-8.1	--

Journal of Chemical Health Risks
www.jchr.org
JCHR (2024) 14(1), 3293-3307 | ISSN:2251-6727

In P. aeruginosa, gyrB (2WYC_B) is the target of a crucial antibiotic, and the docking analysis indicated a significant interaction between Protein (2WYC_B)-ligand (**5a**), forming a single H-bond with the highest binding energy -8.6 Kcal/mol. The interacting residue was HIS-23 (3.23 Å), with ligands. and ten Vander Waals interactions were formed stabilizing the binding affinity between protein-ligand. Further, the standard drugs Ampicillin and Fluconazole were docked to compare and analyze the binding affinity with respective targets. The Fluconazole-1AI9_B complex exhibited binding affinity with residues GLY-23 (2.6 Å) & TRP-27 (3.0 Å), forming two H-bonds, where the Ampicillin-2WYC_B interaction formed single H-bond with the residue ILE-294 (2.3 Å), and Ampicillin-model_1 interaction yielded five H-bonds with residues HIS-118 (2.1 Å), ARG-192 (2.7 Å; 2.4 Å; 2.7 Å) & GLU-602 (2.7 Å). Ampicillin interacted with ARG-192 residue, significantly forming three H-bonds. 2D plots (LigPlot+) were generated to perform the post docking analysis protein-ligand interactions. The results of docking studies with **1AI9_B**, **2WYC_B** and model_1 are as depicted in the **Fig 2**.

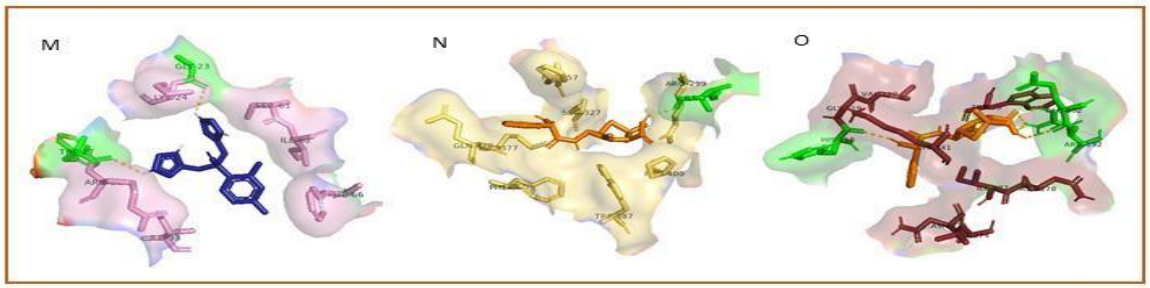

Figure 2. Demonstrates the interaction between **Fluconazole**(blue) with (M) (**1AI9_B**) (lightpink) forming two H-bonds (GLY-23 & TRP-27), (N) **Ampicillin** (orange) interaction with (**2WYC_B**) (yelloworange) with one H-bond (ILE-294) and (O) **Ampicillin** (orange) interaction with (**model_1(B. subtilis**)) (ruby)interaction with five H-bonds (HIS-118, ARG-192 (three H-bonds) & GLU-602.

3.3.2. In silico Docking analysis DNA binding interaction

DNA docking simulation analysis of DNA structure d(CGCGAATTCGCG)2 dodecamer (1BNA) with **5(a-f)** was executed. The ligand **5a and 5b** resulted in the highest docking energy score -7.1 Kcal/mol by forming the three H-bonds with nucleotides DT-8 ((3.14 Å) and (3.30 Å)) and DT-9 (2.99 Å) and five Vander Waals interactions were formed by stabilizing the binding affinity between DNA-**5a** as shown in **Fig.3**. 2D interaction plots were generated to analyze the DNA-ligand interactions. The docking simulation analysis based on AutoDock vina binding energy scores specified a direct correlation with mic (in vitro) values as obtained. The comparative analysis based on the docking scores and the protein-ligand and DNA-ligand interactions with the selected targets obliges to state ligand **5a** exhibits relatively highest antimicrobial activity and **5a** and **5b** exhibits significant DNA binding activity. The results of the analysis are shown in **Table 2.**

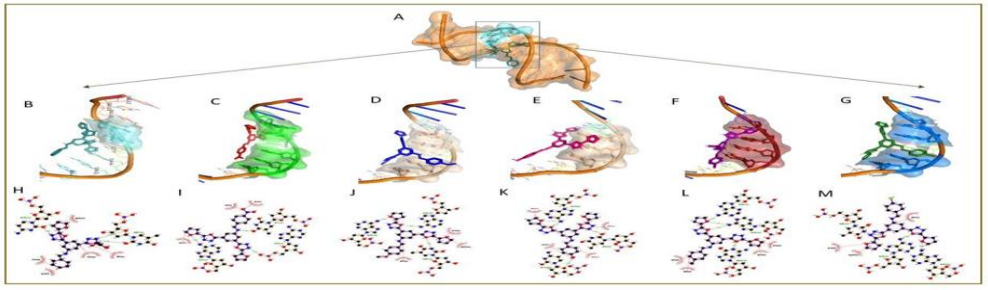

Figure 3. (A) Depiction of the interaction between compounds**(5a-5f)** interacts with DNA helix at supercoiling regions of (B) DT-8, DC-9; (C) DA-5, DA-6, DT-7; (D) DA-5**;** DA-6, DT-8; (E) DA-6, DT-8, DC-11;(F) DG-4, DA-5, DA-6 and (G)DA-5, DA-6, DT-8 with the docking energies of -7.1, -7.1, -6.7, -6.6, -6.8 & -6.8 kcal/mol correspondingly.

Journal of Chemical Health Risks
www.jchr.org
JCHR (2024) 14(1), 3293-3307 | ISSN:2251-6727

Nucleotides DA-5, DA-6 & DT-8 was highly conserved and involved in the DNA-ligand interactions. Compounds **5a, 5b, 5e**and **5f**displayedrelatively crucial binding potential with DNA(1BNA), 2D plots (LigPlot^{+}) of protein-ligands (**5a-5f)** interactions (H-M) is shown with H- bonds and hydrophobic interactions.

Table 2 Depiction of the DNA binding energy scores (AutoDock scores) of **5(a-f)**

DNA binding (BDNA)	Binding Energy (kcal/mol) at rmsd/ub=0 & rmsd/lb=0					
	5a	**5b**	**5c**	**5d**	**5e**	5f
PDB ID: 1BNA	-7.1	-7.1	-6.7	-6.6	-6.8	-6.8

In silico Acute Oral Toxicity analysis

For the prediction of the AOT, the small molecules **5(a-f)** were submitted to DL-AOT in the

.sdf format, and the model type was set to "Regression model and multi-class model." DL- AOT predictions of the individual molecules resulted in predicting the values of resultant consensus models were based on a regression model (log(LD50)) with the unit log(mg/kg). The probably evaluated toxicity levels of **5a-5f** were predicted based on the multi- classification models as shown in **Table 3**. The submitted molecules **5a**, **5b**, and **5e** were classified as "caution," whereas **5c**, **5d**, and **5f** as "none required" based on the Regression model and multi-classification model values predicted. None of the molecules fell under the category of "danger/poison" and "warning." The predicted results signify that all the molecules **5(a-f)** can be considered further as the in-silico predictions suggest the molecules are least or non-toxic subjected to further analysis for confirmation.

Table 3 Evaluated toxicity levels of **5(a-f)** compounds based on DL-AOT prediction.

Model ID	Regression [Value (log(LD50) (log(mg/kg))]	Multi-classification [Label (probability)]	Toxicity Evaluation
5a	3.75	3 (0.62)	
5b	3.76	3 (0.88)	
5c	3.81	4 (0.88))	
5d	3.80	4 (0.92)	
5e	3.81	3 (0.53)	
5f	3.84	4 (0.77)	
5f	3.84	4 (0.77)	

Toxicity: (1) danger/poison (2) warning (3) caution (4) none required

3.4. In vitro antimicrobial screening

3.4.1. Evaluation of minimal inhibitory concentrations (MIC)

The synthesized compounds' MIC taken with dilution ranges from 2.5 to 20 mg/ mL. all the compounds tested shown found effective against Pseudomonas aeruginosa. Compounds 5b, 5d, and 5e showed moderate activity against Bacillus subtilis, and compound 5c was more potent against Escherichia coli. Further among the compound tested compounds, 5c, 5a and 5e showed significant inhibition at MIC 2.5 mg/mL against E. coli and Candida parapsilosis. The MIC results at a concentration of 2.5 mg/mL of the lowest MIC were observed for the compounds 5a, 5c, and 5e exhibit more efficient MIC than other test compounds. Results of MIC are depicted in **Table 4.**

Journal of Chemical Health Risks
www.jchr.org
JCHR (2024) 14(1), 3293-3307 | ISSN:2251-6727

Table 4 In vitro minimum inhibition concentrations of synthesized compound **(5a-g)**

Test Compounds (mg/mL) Test pathogenic microorganisms	**5a**	**5b**	**5c**	**5d**	**5e**	**5f**	5g
Staphylococcus aureus	20	10	20	05	05	10	**20**
Pseudomonas aeruginosa	20	2.5	*	2.5	10	05	*****
Bacillus subtilis	10	05	05	20	05	10	**10**
Escherichia coli	*	10	10	2.5	10	*	**10**
Candida albicans	05	05	10	05	2.5	20	**20**
Candida parapsilosis	**05**	**10**	*****	**2.5**	**05**	**10**	*****

* Indicates values more than 40 mg/mL. The value of each constituent consisted of ± S.E.M. of 03 replicates. ND – Not Defined.

3.4.2. Antimicrobial screening

All compounds tested for their efficiency for having antimicrobial property exhibited a significant zone of inhibition against microorganisms. Synthesized molecule bearing a hetero atom enhances the inhibition of the action of the bacteria and fungi used for the experiment and proved as a potent antimicrobial activity. Antimicrobial results reveal that all the compounds are effective against Bacillus Subtilis, with the zone of inhibition between 20.67 ± 0.33mm to 21.73 ± 1.01 mm, which is almost similar to the Ampicillin drug, which was used as standard which was exhibited a zone of inhibition of 24.36 ± 1.45 mm. Further compounds 5c,5a, and 5e containing phenolic OH, phenyl, and chloro groups found significant against P. aeruginosa, resulting in inhibiting of 19.21 ± 0.33 mm, 19.23 ± 0.96 mm, and 19 ± 17.0 6mm, which was comparably found similar activity with standard drug shown inhibition of 19.67 ± 0.88. Compound 5c with 19± 0.58 mm zone of inhibition moderate action against E. coli. Compare to standard drugs. Compound 5f was found to be effective against fungi Candida albicans used with a zone of inhibition 17.62 ± 0.56. The Rest of the compound is found to be an average action against the microorganism used for the test. The results of the antimicrobial activity revealed synthesized some of the compounds were found to effectively inhibit the action of both bacterial and fungal growth rest were moderately active. Among the test compounds, 5c, 5a, and 5e proved as a significant antimicrobial molecule. The results of the test were shown in **Table 5**.

Table 5 Antimicrobial activity of the synthesized compounds **5(a- f)**

Zone of inhibition (mm) **Compounds**	**Staphylococcus aureus** ATCC 25923	**Bacillus Subtilis** ATCC 6633	**Escherichia coli** ATCC 25922	**Pseudomonas aeruginosa** ATCC 27853	**Candida albicans** ATCC 10231	**Candida parapsilosis** ATCC 90018
5a	16.33 ± 0.56	21.27 ± 1.01	14.67 ± 0.95	19.23 ± 0.96	15.63 ± 1.2	14.67 ± 0.33
5b	25 ± 0.86	21.73 ± 1.01	14.33 ± 1.45	14.67 ± 1.86	12.63 ± 1.13	14.01 ± 0.33

Journal of Chemical Health Risks
www.jchr.org
JCHR (2024) 14(1), 3293-3307 | ISSN:2251-6727

5c	15 ± 1.15	21.46 ± 1.01	19± 0.58	19.51 ± 0.33	16.26 ± 0.58	16.27 ± 1.01	
5d	17.33 ± 0.88	21.33 ± 1.01	15.27 ± 0.5	16.13 ± 1.2	14.67 ± 1.45	16.17 ± 0.95	
5e	22.67 ± 0.88	20.67 ± 0.33	17.83 ± 0.33	19 ± 17.06	14.67 ± 1.86	15.48 ± 2.52	
5f	13.33 ± 1.2	21.33 ± 1.01	16.67 ± 1.45	17.33 ± 0.58	17.62 ± 0.56	17.33 ± 1.01	
Ampicillin	17 ± 1.53	24.36 ± 1.45	26.83 ± 0.88	19.67 ± 0.88	--	--	
Fluconazole	--	--	--	--	19.3 ± 0.33	18.83 ± 1.13	

3.5. DNA interaction experiments

Buffer (5 mM tris (hydroxymethyl) aminomethane with 50 mM NaCl, pH 7.2,) was used to dissolve concentration of CT-DNA. [$C_{(p)}$] was measured at 260 nm (6600 $M^{-1}cm^{-1}$) using its extinction coefficient [**11**]. 260 nm (A_{260}) by 280 nm (A_{280}) to verify the purity level. Were set to evaluate the absorption of CT-DNA at 260 nm. Absence of protein with CT-DNA were confirmed by the proportion of A_{260}/A_{280} which was found in the range of 1.8 to 1.9. Concentration (0 to 100 μM) of DNA was considered to perform the titration by keeping compound concentration constant (0.5 μM). The absorption spectrum was noted for each successive addition of DNA to synthesized 1,3,4-Oxadiazole Schiffs base derivatives **5(b-g)** and contrast (about 10 min). To achieve the constant of intrinsic attachment, K_b:

$$[DNA] / (\varepsilon_a - \varepsilon_f) = [DNA] / (\varepsilon_b - \varepsilon_f) + 1/K_b (\varepsilon_b - \varepsilon_f) \quad (1)$$

where ε_a, ε_f, and ε_b are the apparent, free, and bound compound extinction coefficients, respectively. A plot of $[DNA]/(\varepsilon_a - \varepsilon_f)$ versus [DNA] gave a slope of $1/(\varepsilon_b - \varepsilon_f)$ and an intercept y equal to $1/K_b(\varepsilon_b - \varepsilon_f)$, where K_b is the ratio of the slope to the intercept y. Result are depicted in the **Figure 4 – Figure 6.** DNA cleavage experiments

For the gel electrophoresis analysis, supercoiled pUC19 DNA has been treated with compounds (**5b-g**). The study was conducted in 2 mL quantity comprising pUC19 DNA of 5 μmol/L phosphate solution mixed with 10 μmol NaCl, pH 7.4, with distinct compounds level (25–50 μmol/L). The test sample was mixed with 0.5 mL of 0.25% bromophenol yellow, 0.25% xylene cyanol FF, 30% glycerol and the sample was further examined using 1% agarose electrophoresis by submerging the gel in Tris-borate buffer (1 μmol/L EDTA, 45 μmol/L Tris-borate) and running at 50 V for 2.5 h. The untreated pUC19 DNA was kept as parallel control. The gel was dyed with ethidium bromide (1 μg/mL) and then photographed under UV light [**12**]. The cleavage pattern of the compound shown in the **Figure 7.**

4. Conclusion

Novel 1,3,4- Oxadiazole-based Schiff's base derivatives synthesized are characterized by the IR, NMR, and Mass spectral studies, and the results are found in good agreement with the molecular structure. In silico molecular docking studies, for the PDB structures of the protein targets exhibit compounds **5(a-f)** having significant binding efficiency ranging between -9.9 to -10.8 against B. subtilis and **-8.5** to **-8.8** against P. aeruginosa are substantial. Further, the in vitro antimicrobial studies reveal, compounds **5c, 5a,** and **5e** to be more potent antimicrobial compounds. DNA binding and cleavage studies have shown compounds **5b, 5d,** and **5g** have reliable binding interactions with DNA helix; among the synthesized compounds screened for DNA cleavage, compound **5g** was observed to be the most effective nuclease mimic in comparison to compounds **5b** and **5d** in terms of substituents. The results of the biological activity screening conclude that synthesized novel compound proved as a potent antimicrobial agent. DNA docking study concludes **5b, 5d,** and **5g** can form hydrogen bonds through its minor

groove, which can most effectively inhibit the action of DNA activity.

Declarations Acknowledgements

Authors are thankful to Manipal Academy of Higher Education, Manipal, Karnataka, INDIA. for the computational facilities. Authors remain thankful to Chairman and the members of S.V.M.V.V Sangha Ilkal, Karnataka, INDIA. Authors express their thanks to RNS Institute of Technology, Bangalore and Ranichannamma University Belagavi, Karnataka, INDIA. for providing laboratory facilities to carry out the experiments.

Funding

This research did not receive any specific grant from funding agencies in the public, commercial, or not-for-profit sectors.

Conflict of interest

The authors declare no competing interests.

Data availability

The datasets generated during and/or analysed during the current study are available from the corresponding author on reasonable request.

Reference

1. Shridhar AH, Keshavayya J, Peethambar SK, Joy Hoskeri H. Synthesis and biological activities of Bis alkyl 1,3,4-oxadiazole incorporated azo dye derivatives. Arabian Journal of Chemistry 2016;9S1643–S1648. https://doi.org/10.1016/j.arabjc.2012.04.018
2. Guimarães CRW, Boger DL, Jorgensen WL. Elucidation of Fatty Acid Amide Hydrolase Inhibition by Potent α-Ketoheterocycle Derivatives from Monte Carlo Simulations. J Am Chem Soc 2005;127(49):17377–17384. https://doi.org/10.1021/ja055438j.
3. Zheng Z, Liu Q, Kim W, Tharmalingam N, Fuchs BB, Mylonakis E. Antimicrobial activity of 1,3,4-oxadiazole derivatives against planktonic cells and biofilm ofStaphylococcus aureus. Future Medicinal Chemistry 2018;10(3):283–296. https://doi.org/10.4155/fmc-2017-0159
4. Rajak H, Kharya MD, Mishra P. Synthesis of Some Novel Oxadiazole and Oxadiazoline Analogues for Their Antiinflammatory Activity. YAKUGAKU ZASSHI 2007;127(10):1757–1764. https://doi.org/10.1248/yakushi.127.1757
5. Kumar A, D'Souza SS, Gaonkar SL, Rai KML, Salimath BP. Growth inhibition and induction of apoptosis in MCF-7 breast cancer cells by a new series of substituted- 1,3,4-oxadiazole derivatives. Invest New Drugs 2008;26(5):425–435. https://doi.org/10.1007/s10637-008-9116-5
6. Chen C-J, Song B-A, Yang S, Xu G-F, Bhadury PS, Jin L-H, Hu D-Y, Li Q-Z, Liu F, Xue W, Lu P, Chen Z. Synthesis and antifungal activities of 5-(3,4,5- trimethoxyphenyl)-2-sulfonyl-1,3,4-thiadiazole and 5-(3,4,5-trimethoxyphenyl)-2-sulfonyl-1,3,4-oxadiazole derivatives. Bioorganic & Medicinal Chemistry 2007;15(12):3981–3989.https://doi.org/10.1016/j.bmc.2007.04.014.
7. Hassan MF, Rauf A. Synthesis and multi-spectroscopic DNA binding study of 1,3,4-oxadiazole and 1,3,4-thiadiazole derivatives of fatty acid. Spectrochimica Acta Part A: Molecular and Biomolecular Spectroscopy 2016;153510–516. https://doi.org/10.1016/j.saa.2015.09.005.
8. Abdelrehim EM. Synthesis and Screening of New [1,3,4]Oxadiazole, [1,2,4]Triazole, and [1,2,4]Triazolo[4,3-b][1,2,4]triazole Derivatives as Potential Antitumor Agents on the Colon Carcinoma Cell Line (HCT-116). ACS Omega 2021;6(2):1687–1696. https://dx.doi.org/10.1021/acsomega.0c05718
9. Mishra P, Rajak H, Mehta A. Synthesis of Schiff bases of 2-amino-5-aryl-1, 3, 4- oxadiazoles and their evaluation for antimicrobial activities. J Gen Appl Microbiol 2005;51(2):133–141. https://doi.org/10.2323/jgam.51.133.
10. Ullah H, Rahim F, Taha M, Hussain R, Tabassum N, Wadood A, Nawaz M, Mosaddik A, Imran S, Wahab Z, Miana GA, Kanwal, Khan KM. Aryl-oxadiazole Schiff bases: Synthesis, α-glucosidase in vitro inhibitory activity and their in silico studies. Arabian Journal of Chemistry 2020;13(4):4904–4915. https://doi.org/10.1016/j.arabjc.2020.01.005.
11. Shridhar AH, Keshavayya J, Peethambar SK, Joy Hoskeri H. Synthesis and biological activities of Bis alkyl 1,3,4-oxadiazole incorporated azo dye derivatives. Arabian Journal of Chemistry 2016;9S1643–S1648. http://dx.doi.org/10.1016/j.arabjc.2012.04.018
12. Vinay Kumar B, Naik HSB, Girija D, Sharath N,

Sudeep HV, Joy Hoskeri H. Synthesis and Biological Evaluation of New Tetra-aza Macrocyclic Scaffold Constrained Oxadiazole, Thiadiazole and Triazole Rings. Arch Pharm Pharm Med Chem 2011;345(3):240–249. https://doi.org/10.1002/ardp.201100181

13. Abdel-Rahman LH, Abu-Dief AM, Shehata MR, Atlam FM, Abdel-Mawgoud AAH. Some new Ag(I), VO(II) and Pd(II) chelates incorporating tridentate imine ligand: Design, synthesis, structure elucidation, density functional theory calculations for DNA interaction, antimicrobial and anticancer activities and molecular docking studies. Appl Organometal Chem 2019;33(4): e4699. https://doi.org/10.1002/aoc.4699
14. Walum E. Acute oral toxicity. Environmental Health Perspectives 1998;106(suppl 2):497–503. http://dx.doi.org/10.1289/ehp.98106497
15. Yang H, Sun L, Li W, Liu G, Tang Y. In Silico Prediction of Chemical Toxicity for Drug Design Using Machine Learning Methods and Structural Alerts. Front. Chem. Frontiers Media SA; 2018;6. http://dx.doi.org/10.3389/fchem.2018.00030
16. Xu Y, Pei J, Lai L. Deep Learning Based Regression and Multiclass Models for Acute Oral Toxicity Prediction with Automatic Chemical Feature Extraction. J. Chem. Inf. Model. American Chemical Society (ACS); 2017;57(11):2672–85. http://dx.doi.org/10.1021/acs.jcim.7b00244
17. DeJarnette C, Luna-Tapia A, Estredge LR, Palmer GE. Dihydrofolate Reductase Is a Valid Target for Antifungal Development in the Human Pathogen Candida albicans. Mitchell AP, editor. mSphere. American Society for Microbiology; 2020;5(3). http://dx.doi.org/10.1128/mSphere.00374-20
18. Otzen T, Wempe EG, Kunz B, Bartels R, Lehwark-Yvetot G, Hänsel W, et al. Folate-Synthesizing Enzyme System as Target for Development of Inhibitors and Inhibitor Combinations against Candida albicansSynthesis and Biological Activity of New 2,4-Diaminopyrimidines and 4‘-Substituted 4-Aminodiphenyl Sulfones. J. Med. Chem. American Chemical Society (ACS); 2003;47(1):240–53. http://dx.doi.org/10.1021/jm030931w
19. Murugavel S, Jacob Prasanna Stephen CS, Subashini R, AnanthaKrishnan D. Synthesis, structural elucidation, antioxidant, CT-DNA binding and molecular docking studies of novel chloroquinoline derivatives: Promising antioxidant and anti- diabetic agents. Journal of Photochemistry and Photobiology B: Biology. Elsevier BV; 2017;173:216–30. http://dx.doi.org/10.1016/j.jphotobiol.2017.05.043
20. Rezki N, Al-blewi FF, Al-Sodies SA, Alnuzha AK, Messali M, Ali I, et al. Synthesis, Characterization, DNA Binding, Anticancer, and Molecular Docking Studies of Novel Imidazolium-Based Ionic Liquids with Fluorinated Phenylacetamide Tethers. ACS Omega. American Chemical Society (ACS); 2020;5(10):4807–15. http://dx.doi.org/10.1021/acsomega.9b03468
21. Fathima SSA, Meeran MMS, Nagarajan ER. Synthesis, characterization and biological evaluation of novel 2,2′-((1,2-diphenylethane-1,2-diylidene)bis(azanylylidene))bis(pyridin-3-ol)and metal complexes: molecular docking and in silico ADMET profile. Struct Chem. Springer Science and Business Media LLC; 2019;31(2):521–39. http://dx.doi.org/10.1007/s11224-019-01425-7
22. Frère J-M, Page MG. Penicillin-binding proteins: evergreen drug targets. Current Opinion in Pharmacology. Elsevier BV; 2014 Oct;18:112–9. http://dx.doi.org/10.1016/j.coph.2014.09.012
23. Zapun A, Contreras-Martel C, Vernet T. Penicillin-binding proteins and β-lactam resistance. FEMS Microbiol Rev. Oxford University Press (OUP); 2008;32(2):361–
85. http://dx.doi.org/10.1111/j.1574-6976.2007.00095.x
24. Lee SA, Gallagher LA, Thongdee M, Staudinger BJ, Lippman S, Singh PK, et al. General and condition-specific essential functions of Pseudomonas aeruginosa. Proc Natl Acad Sci USA. Proceedings of the National Academy of Sciences; 2015;112(16):5189–94. http://dx.doi.org/10.1073/pnas.1422186112
25. Tari LW, Li X, Trzoss M, Bensen DC, Chen Z, Lam T, et al. Tricyclic GyrB/ParE (TriBE) Inhibitors: A New Class of Broad-Spectrum Dual-Targeting Antibacterial Agents. Mayer C, editor. PLoS ONE. Public Library of Science (PLoS); 2013;8(12):e84409. http://dx.doi.org/10.1371/journal.pone.0084409
26. Waterhouse A, Bertoni M, Bienert S, Studer G, Tauriello G, Gumienny R, et al. SWISS-MODEL: homology modelling of protein structures and complexes. Nucleic Acids Research. Oxford University Press (OUP); 2018;46(W1):W296–303.

http://dx.doi.org/10.1093/nar/gky427

27. Benson G. Editorial. Nucleic Acids Research. Oxford University Press (OUP); 2013;41(W1):W1–2. http://dx.doi.org/10.1093/nar/gkt559
28. Sahoo M, Jena L, Rath SN, Kumar S. Identification of Suitable Natural Inhibitor against Influenza A (H1N1) Neuraminidase Protein by Molecular Docking. Genomics Inform. Korea Genome Organization; 2016;14(3):96. http://dx.doi.org/10.5808/GI.2016.14.3.96
29. Trott O, Olson AJ. AutoDock Vina: Improving the speed and accuracy of docking with a new scoring function, efficient optimization, and multithreading. J. Comput. Chem. Wiley; 2009;NA-NA. http://dx.doi.org/10.1002/jcc.21334
30. O'Boyle NM, Banck M, James CA, Morley C, Vandermeersch T, Hutchison GR. Open Babel: An open chemical toolbox. J Cheminform. Springer Science and Business Media LLC; 2011;3(1). http://dx.doi.org/10.1186/1758-2946-3-33
31. DeLano WL. Pymol: An open-source molecular graphics tool. CCP4 Newsletter on protein crystallography. 2002;40(1):82-92.
32. Laskowski RA, Swindells MB. LigPlot+: Multiple Ligand–Protein Interaction Diagrams for Drug Discovery. J. Chem. Inf. Model. American Chemical Society (ACS); 2011;51(10):2778–86. http://dx.doi.org/10.1021/ci200227u
33. Islam M, Alam M, Choudhury M, Kobayashi N, Ahmed M. Determination of minimum inhibitory concentration (MIC) of cloxacillin for selected isolates of methicillin-resistant Staphylococcus aureus (MRSA) with their antibiogram. Bangl J Vet Med 1970;6(1):121–126. https://doi.org/10.3329/bjvm.v6i1.1350
34. Smith S, Bamidele M, Goodluck H, Fowora M, Omonigbehin E, Oper B, Aboaba O. Antimicrobial susceptibilities of salmonellae isolated from food handlers and cattle in Lagos, Nigeria. Int J Health Res;2(2). https://doi.org/10.4314/ijhr.v2i2.55421
35. Lehrer RI, Rosenman M, Harwig SSSL, Jackson R, Eisenhauer P. Ultrasensitive assays for endogenous antimicrobial polypeptides. Journal of Immunological Methods 1991;137(2):167–173. https://doi.org/10.1016/0022-1759(91)90021-7
36. Vidyavathi GT, Vinay Kumar B, Aravinda T, Hani U. Cashew nutshell liquid catalyzed green chemistry approach for synthesis of a Schiff base and its divalent metal complexes: molecular docking and DNA reactivity. Nucleosides, Nucleotides & Nucleic Acids 2021;40(3):264–287. https://doi.org/10.1080/15257770.2020.1868502
37. Neelakantan MA, Balamurugan K, Balakrishnan C, Subha L. Interaction of Amino Acid Schiff Base Metal Complexes with DNA/BSA Protein and Antibacterial Activity: Spectral Studies, DFT Calculations and Molecular Docking Simulations. Appl Organometal Chem 2018;32(4):e4259. https://doi.org/10.1002/aoc.4259
38. Abdel-Rahman LH, Adam MS, Abu-Dief AM, Ahmed HE-S, Nafady A. Non-Linear Optical Property and Biological Assays of Therapeutic Potentials Under In Vitro Conditions of Pd(II), Ag(I) and Cu(II) Complexes of 5-Diethyl amino-2-({2-[(2- hydroxy-Benzylidene)-amino]-phenylimino}-methyl)-phenol. Molecules 2020;25(21):5089. https://doi.org/10.3390/molecules25215089
39. Mohanraj M, Ayyannan G, Raja G, Jayabalakrishnan C. Synthesis, characterization, DNA binding, DNA cleavage, antioxidant and in vitro cytotoxicity studies of ruthenium(II) complexes containing hydrazone ligands. Journal of Coordination Chemistry 2016;69(23):3545–3559. https://doi.org/10.1080/00958972.2016.123570